The 2009 IEEE/RSJ International Conference on
Intelligent Robots and Systems
October 11-15, 2009 St. Louis, USA

Execution of Dynamic Maneuvers for Unmanned Ground Vehicles Using Variable Internal Inertial Properties

Chenghui Nie, Simo Cusi Van Dooren, Jainam Shah, and Matthew Spenko, *Member, IEEE*

***Abstract*— An Unmanned Ground Vehicle (UGV) capable of executing controlled sliding and sharp turns without a significant decrease in velocity would have superior utility in field operations compared to a standard UGV. Such a vehicle would be better able to maneuver in tight corridors, avoid obstacles detected at short range, and minimize its time in dangerous situations. This paper presents theoretical analysis and experimental results of a UGV executing extreme dynamic maneuvers by altering its internal mass and inertial properties during locomotion. The behaviors are accomplished by shifting the location of the UGV's center of mass while executing a turn. This modifies the normal force acting on the wheels, which in turn modifies their maximum lateral traction forces.**

I. Introduction

An Unmanned Ground Vehicle (UGV) must maximize its agility to increase its effectiveness in field operations. Agility is defined here as the ability to quickly change directions without a significant loss in speed. Maximizing a UGV's agility will allow it to travel at higher speeds and reduce its exposure to dangerous situations. The UGV will be better equipped to actively avoid hazards, especially those detected at close range. It will also be able to maneuver in tight corridors and confined spaces. Conversely, a vehicle that is agile has the ability to safely recover from unwanted dynamic maneuvers that might result from improperly identified or unforeseen terrain conditions.

Almost all UGVs have the ability to traverse or avoid obstacles, but most, if not all, lack agility. This is partly because a majority of the previous research concerning UGVs focuses on operation at low speeds [1], [2]. Some work has been done in investigating the dynamic behavior of small robots [3], [4]; but again, little focus is placed on turning. For larger vehicles, most notably automobiles, there has been significant research in understanding cornering dynamics [5] and yaw stability control [6] in the context of maintaining stability and safety, but very little for extreme dynamic maneuvers [7]. Some UGVs are kinematically configured to be inherently agile, notably omnidirectional vehicles that use Mecanum or similar type wheels [8]. However, these UGVs are restricted to clean, smooth, surfaces since their slender specialized wheels do not perform well in dusty, dirty, and uneven terrains. This limits their effectiveness in practical field operations.

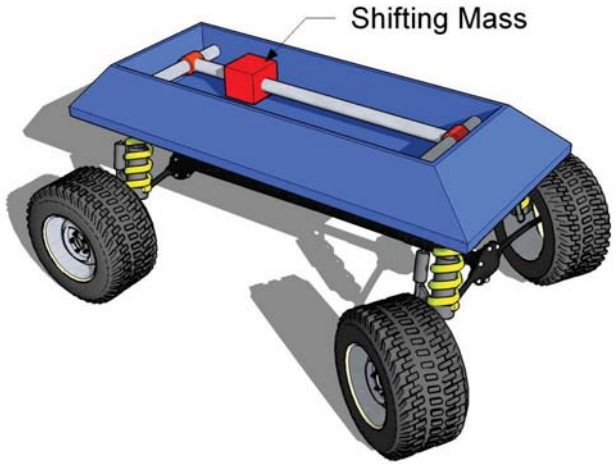

Fig. 1. Illustration of an agile UGV with the capabilities to modify the location of its center of mass.

This paper presents a novel technique to increase the agility of UGVs by adjusting their inertial properties to create controlled skidding or quickly and easily end unwanted skidding. By adjusting these properties while a vehicle is in motion, it is possible to execute highly dynamic maneuvers that would otherwise require complicated control techniques. Specifically, the location of the UGV's center of mass (c.o.m.) is shifted during operation to modify the normal forces acting on the tires (see Fig. 1). This is fundamentally different from the popular Electronic Stability Control (ESC) found on most modern passenger vehicles. ESC commonly utilizes differential braking on individual tires to help stabilize the yaw rate of the vehicle. Furthermore, while a standard (no active DOF to change the location of the c.o.m.) vehicle may have its mass distribution tuned for a specific application or terrain, its parameters are essentially fixed, which fundamentally limits the vehicle's performance. The approach presented here changes the system at its most basic level, allowing a vehicle to essentially change its dynamic properties during locomotion.

Practically this can be accomplished by shifting the payload of the vehicle along with any components that are not part of the drive train or suspension system (e.g. batteries, fuel, and on-board electronics). The energy to accomplish this would be very small, around $40J$ for a $20kg$ vehicle that

This work was supported through startup funds provided by the Illinois Institute of Technology.

M. Spenko is on the Faculty of the Mechanical, Materials, and Aerospace Engineering Department, Illinois Institute of Technology, Chicago, IL 60616, USA. mspenko@iit.edu

C.H Nie is a PHD student in the Mechanical, Materials, and Aerospace Engineering Department, Illinois Institute of Technology. cnie5@iit.edu

S. Cusi Van Dooren was a visiting student at the Illinois Institute of Technology. scusiva@iit.edu

J. Shah is with the Mechanical, Materials, and Aerospace Engineering Department, Illinois Institute of Technology. jshah60@iit.edu

shifts half of its mass a distance of $0.5m$ in $0.5s$. This would not significantly impact the mission duration of vehicle.

Some robots do reconfigure their internal structure, but most if not all do so only to change their form of locomotion or kinematic configuration (see [9] for an overview). Other UGVs change the location of their center of mass to decrease the chance of rollover [10]. To the authors' knowledge, no mobile ground robot modifies its internal structure in order to change its dynamic properties.

In passenger vehicles, wheel slip is traditionally detrimental and is avoided, but expert human drivers have been able to use it to their advantage when trying to execute extreme dynamic maneuvers, often referred to as "drifting." Drifting is defined here as occurring when the slip angle of the vehicle, β, the angle of the vector sum of the vehicle's longitudinal and sideslip velocity, is larger than $10\,^{\circ}$.

There are a number of complicated techniques used by professional drivers to induce drifting. These include locking the rear wheels with the clutch depressed, accelerating hard at a corner exit, down-shifting without rev-matching or braking to temporarily lock the rear wheels, rapidly disengaging the clutch to shock the power-train and temporarily upset the car's balance, and braking into a corner to cause the weight to shift to the front of the vehicle. These approaches would require complicated control algorithms and many would not be suitable to small man-portable or man-packable UGVs that do not possess the necessary transmission. Furthermore, the techniques can easily damage a vehicle's power train.

The commonality among the methods is that they either lock the wheels or upset the balance of the vehicle (by taking advantage of the suspension properties to shift the normal force acting on the tires) in an attempt to decrease traction on the rear wheels such that the centripetal force of the vehicle is greater than the friction force acting on the wheels. However, these techniques can be greatly simplified for unmanned ground vehicles by introducing a degree of freedom that shifts the vehicle's payload in order to change the location of the center of mass. If this dynamic behavior can be controlled, then the UGV can be considered agile.

This paper specifically focuses on Ackerman-type steered vehicles, although the concepts are applicable to skid-steered or legged vehicles as well. Section II addresses cornering dynamics, and Section III presents experimental results that illustrate the desired behavior.

II. Ground Vehicle Cornering Dynamics

This section provides a theoretical foundation to describe how a vehicle's cornering dynamics are related to the location of its mass center. First, vehicle cornering geometry is described. Second, a static force model of the vehicle is presented. Third, a tire model appropriate for large slip angles is shown. Last, the three models are combined to demonstrate how shifting the center of mass location from the rear to the front of a vehicle will allow the vehicle to execute sharp turns at a lower speed than it could otherwise.

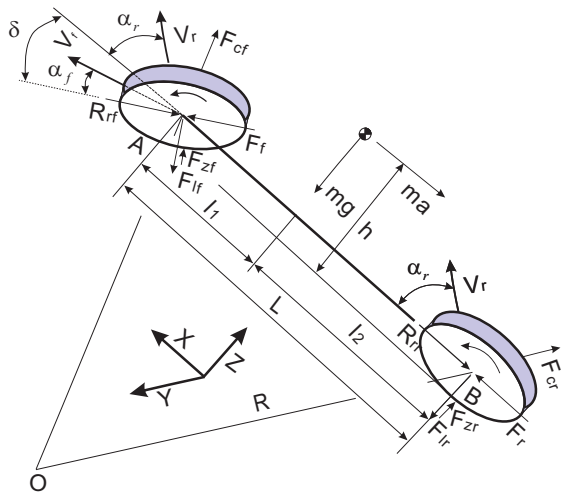

Fig. 2. Single-track model for an Ackerman-steer ground vehicle.

A. Vehicle Cornering Geometry

Ackerman-type wheeled ground vehicles will exhibit one of three types of steady-state cornering behaviors: under-, over-, or neutral-steering [5]. A neutrally steered vehicle does not need to change its steering angle in order to maintain a constant radius curve while increasing forward velocity. An over- or under-steered vehicle must decrease or increase its steering angle respectively. Using the single-track model (see Fig. 2), this relationship is described by the steering angle, δ, required to maintain a turn of radius R:

$$\delta = L/R + \alpha_f - \alpha_r \tag{1}$$

where L is the vehicle wheelbase and $\alpha_{f,r}$ are the front and rear slip angles, defined as the difference between the direction a wheel is oriented and the direction it is traveling [5]. For small slip angles, it has been shown that the lateral force acting on a tire is linearly proportional to the slip angle; however for larger angles, this relationship does not hold and a more sophisticated tire model must be used [6].

B. Vehicle Model

The major external forces acting on vehicle are shown in Fig. 2. In the longitudinal direction, they include the rolling resistance of the rear and front tires, R_{rr} and R_{rf}, and the tractive force of the rear and front tires, F_r and F_f. For a rear-wheel-drive vehicle, $F_f = 0$. In the lateral direction, the forces include the lateral force for the front and rear tires, F_{lf} and F_{lr}, the centripetal force of the front and rear wheel, F_{cf} and F_{cr}, and normal forces F_{zf} and F_{zr}.

The normal forces acting on the rear and front tires are given as:

$$F_{zr} = \frac{mgl_1 + mah}{L} \tag{2}$$

$$F_{zf} = \frac{mgl_2 - mah}{L} \tag{3}$$

where m is the vehicle mass, g is gravity, l_1 is the length from the center of mass to the front axle, l_2 is the length from the center of mass to the rear axle, h is the height of the center of mass, and a is the longitudinal acceleration of the UGV. The lateral forces acting on the rear and front tires are given as:

$$F_{lr} = F_{cr}\cos\alpha_r \tag{4}$$

$$F_{lf} = \frac{F_{cf}\cos(\delta-\alpha_f)}{\cos\delta} + R_{rf}\tan\delta \tag{5}$$

where $F_{cf,r} = m_{f,r}V^2/R$ and $m_{f,r}$ is the portion of the mass acting on the front and rear tires respectively.

The longitudinal force acting on the rear tire is given as:

$$\begin{aligned} F_r = {} & R_{rr} + F_{cr}\sin\alpha_r + F_{lf}\sin\delta + R_{rf}\cos\delta \\ & - F_{cf}\sin(\delta-\alpha_f) + ma \end{aligned} \tag{6}$$

Compared to the traction forces, the rolling resistances are small and are assumed to be zero. It is also assumed that vehicle is operating at a constant velocity and thus the lateral force and tractive force of rear wheel can be written as:

$$F_{lr} = \frac{m_r V^2\cos\alpha_r}{R} \tag{7}$$

$$F_r = \frac{V^2}{R}(m-m_r)\,c + \frac{V^2}{R}m_r\sin\alpha_r \tag{8}$$

where $c = \tan\delta\cos(\delta-\alpha_f) - \sin(\delta-\alpha_f)$

C. Tire Model for Large Slip Angles

For this analysis, we employ the Analytical Elastic Foundation Tire Model, which has been shown to be accurate for large slip angles [6]. Based on the model, the lateral force acting on a wheel, F_y, is given as:

$$F_y = \mu F_z\left(1-\left(1-\frac{4a^2bk}{3\mu F_z}\tan\alpha\right)^3\right) \tag{9}$$

where μ is the traction coefficient, F_z is the normal force acting on the tire, $2a$ is the length of contact patch, $2b$ is the width of tire, k is the lateral stiffness of the tire per unit area, and α is the slip angle.

Combining (4), (5) and (9) yields both the front and rear slip angles:

$$tan\alpha_r = \left[\left(\frac{V^2}{\mu Rg}cos\alpha_r - 1\right)^{\frac{1}{3}} + 1\right]\times\frac{16P_0^2b\mu}{3m_rgk} \tag{10}$$

$$tan\alpha_f = \left[\left(\frac{V^2\cos(\delta-\alpha_f)}{\mu Rg\cos\delta} - 1\right)^{\frac{1}{3}} + 1\right]\times\frac{16P_0^2b\mu}{3(m-m_r)gk} \tag{11}$$

where $P_0 = 3F_z/8ab$.

By combining (7), (8), (10), and (11) we can find the ratio of the total forces acting on the tire from the road, $F_{total} = \sqrt{F_r^2 + F_{lr}^2}$, to the normal force acting on the tire. From this relationship, note that F_{total}/F_z is a function of both velocity and mass over the tire. This relationship can describe when a vehicle will lose traction based on its mass distribution and forward velocity. For example, based on the parameters shown in Table I, the relationship between slipping, mass distribution, and velocity can be shown in Fig. 3. The parameters are based on the design of a second experimental system (see Section IV-B).

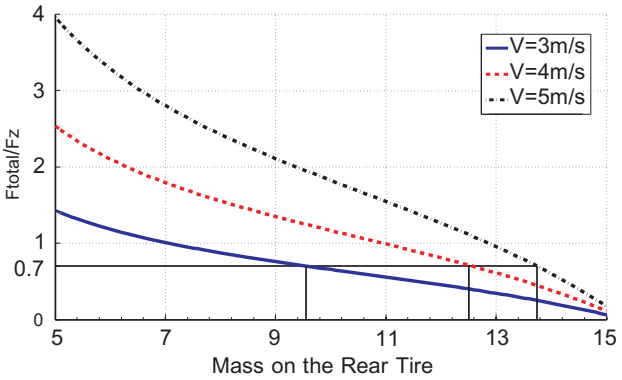

Fig. 3. Ratio between total friction and normal force acting on a wheel as a function of mass for three respective velocities. When the ratio is greater than 0.7 in this example the UGV will begin to drift.

TABLE I
PARAMETERS USED TO ILLUSTRATE SIDESLIP BEHAVIOR

Parameter	Value
steering angle	20°
P_0	2×10^5 (30psi)
mass	20 kg
μ	0.7
k	$2.4\times10^9 N/m^3$

III. Experimental Results

A. Experimental Setup and Procedure

Fig. 4 shows the initial experimental UGV. A second, UGV with a more sophisticated mass shifting mechanism and position measurement system is currently being designed; however, despite its simplicity, the current UGV provides

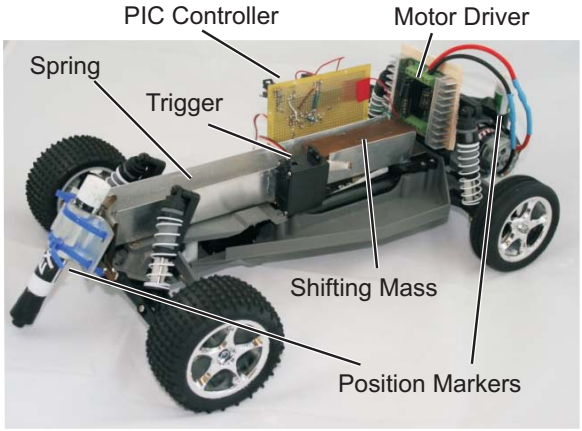

Fig. 4. Vehicle setup

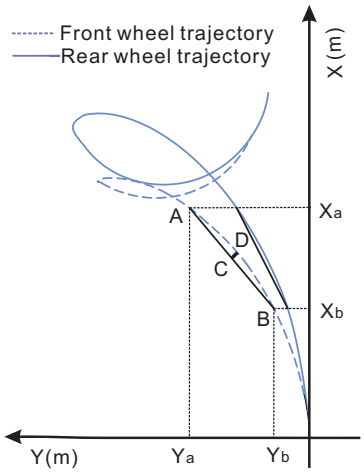

Fig. 5. Data measurement procedure

insightful results demonstrating the validity of this approach. The system is based on a front-wheel steered, rear-wheel driven radio controlled car with a total mass of $2kg$. The UGV can shift a series of masses ranging from 0.25 to $2kg$ along the length of the vehicle. The shifting mass' nominal position is located near the rear of the UGV. The mass is spring-loaded ($k = 0.21N/mm$) and held in place with a trigger mechanism actuated by a servo. The total length of travel is 170mm or 60.7% of the wheelbase. As an example, when a $0.5kg$ mass shifts to the front, the normal force acting on the front and rear wheels changes from 1.5 to $6N$.

The UGV utilizes a PIC chip to control the steering angle, velocity, and trigger position. The velocity is controlled open-loop while the steering and trigger are position controlled and actuated via standard radio controlled servos.

Measurement of the UGV's position is performed with two markers positioned in the front and rear of the vehicle (see Fig 5). The system proved to be simple and effective, and the drag produced by markers had negligible effect on the UGV's trajectory. The future vehicle will employ a Novatel SPAN-CPT GPS/Inertial Measurement Unit so that experiments can be run on a wider range of surfaces and more accurate position measurements can be taken.

Figure 5 illustrates the trajectory measurement process. The two markers trace the trajectory of the front and rear of the vehicle respectively. A line, $\overline{BCA}$, is drawn between two points on the same trajectory that lie a distance $10cm$ apart along the X-axis. Point D is the closest point on that trajectory to the midpoint, C. Points A, B, and D are assumed to lie on the same circle and the radius of curvature for point D is given as:

$$R = \frac{l_{AB}^2}{2l_{CD}} + \frac{l_{CD}}{2} \approx \frac{l_{AB}^2}{2l_{CD}} \tag{12}$$

B. Characterizing the Vehicle Response

Initially, the UGV response with the mass located at the front of the vehicle was recorded in order to characterize the vehicle's behavior. Fig. 6 shows the trajectory when a

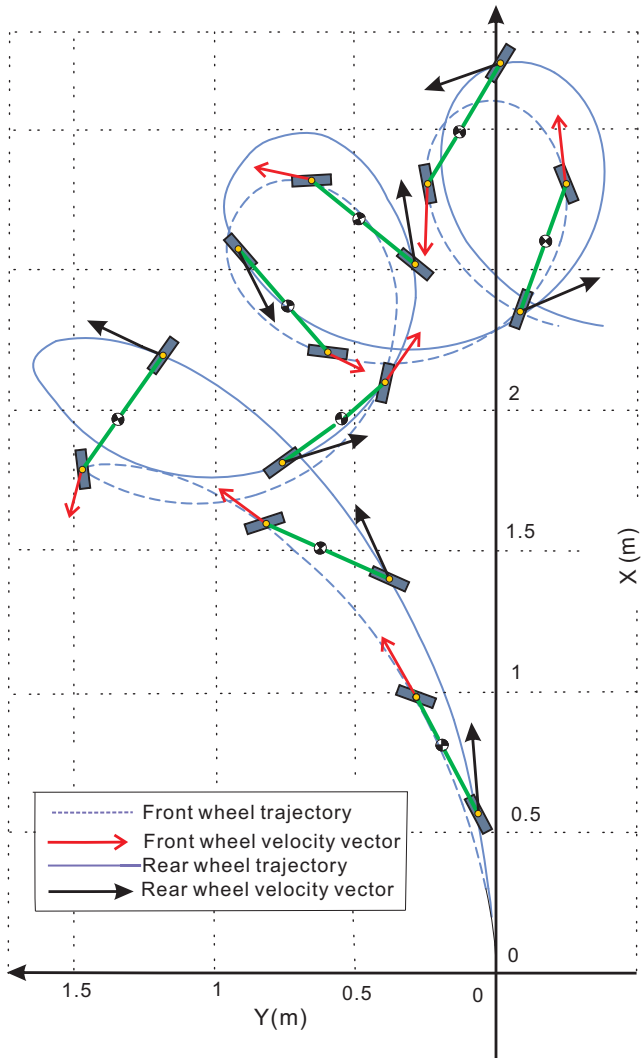

Fig. 6. Vehicle trajectory with a $1kg$ mass located at the front of the vehicle.

$1kg$ mass is located on the front of the UGV. The vehicle is given a constant steering angle and velocity input. If the mass were located over the rear wheels, the UGV would follow a circular path with a radius of curvature defined by its steering angle. This trajectory is not shown.

In this configuration, the velocity is sufficient such the rear wheels slip and the vehicle begins to drift when the centripetal force on the rear tires is greater than the lateral force. Fig. 7 demonstrates how the slip angles of the front and rear wheels change as a function of the recorded data point. Note that after drifting, the UGV recovers and continues at its former yaw rate and then periodically performs similar drifting maneuvers. It is hypothesized that although the vehicle is maintaining close to its steady state velocity, some decrease in velocity is unavoidable since the vehicle is rear wheel drive and the wheels cannot generate enough longitudinal traction. As the UGV exits the drifting behavior it increases its velocity until the centripetal force exceeds the lateral tire force and the drifting behavior is repeated.

Figs. 8 and 9 illustrate the variation in vehicle behavior as

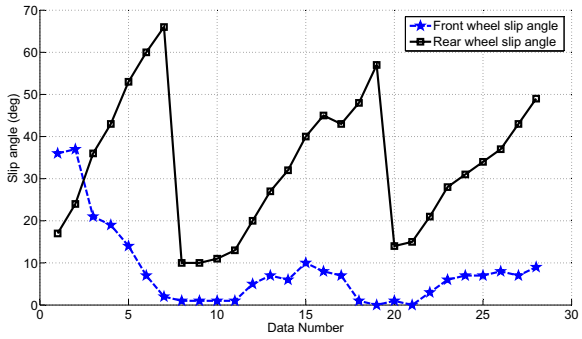

Fig. 7. Slip angle of front wheel and rear wheels when a $1kg$ mass is located at the front.

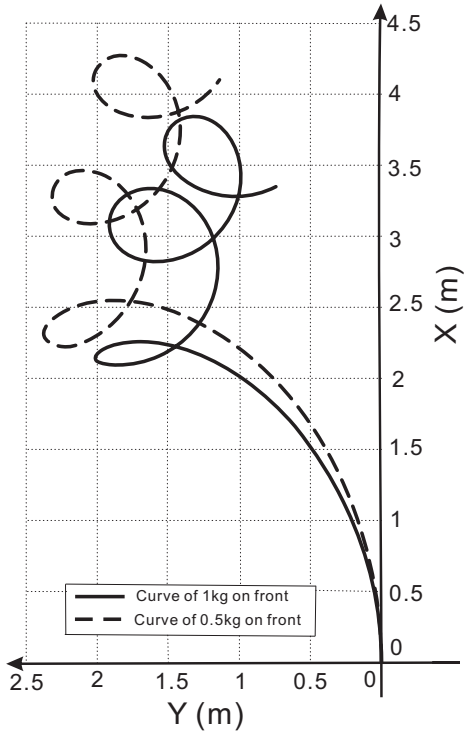

Fig. 8. Comparison of vehicle trajectory for two vehicles. The first has a $1kg$ mass located at the front of the vehicle and the second has a $0.5kg$ mass.

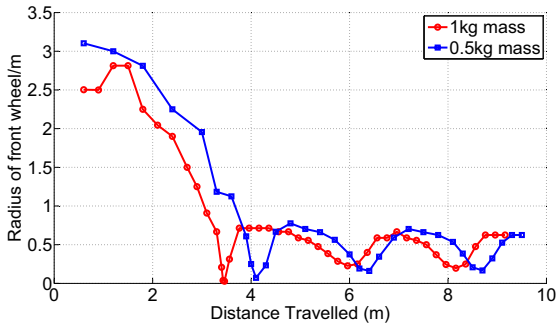

Fig. 9. Comparison of the radius of curvature for two vehicles. The first has a $1kg$ mass located at the front of the vehicle and the second has a $0.5kg$ mass.

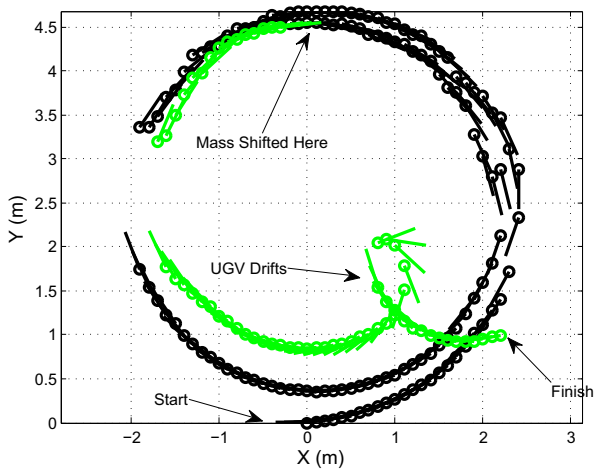

Fig. 10. Trajectory of the vehicle as the mass is shifted from the rear to the front of the vehicle, v = 3 m/s $\delta = 15\,^{\circ}$. The circles represent the front of the UGV, and the lines represent the UGV body. Note that the gap in data located around $X = -2m$ is a result of the measurement procedure and in no way affected the outcome of the experiment.

the mass on the front of the vehicle is increased from 20% of the total mass to 33% of the total mass. All other parameters are kept constant between the two experiments. Note that the trial with the larger mass generates tighter turns, indicating that larger percentage of mass that can be transfered during operation, the more agile the vehicle will be. However, a higher percentage of mass being moved may cause additional issues pertaining to vehicle stability during the actual mass shifting operation, an issue that will be addressed in future work.

C. Execution a Mass Shift During Locomotion

Fig. 10 demonstrates the behavior of the UGV when the mass is shifted from the rear of the vehicle to the front during a steady-state turn. The UGV trajectory consists of a constant steering angle and constant velocity input. Sufficient time is given before the trigger is released to ensure that the vehicle has obtained a steady-state velocity. After the vehicle has reached a steady-state velocity, the trigger is released causing a $0.5kg$ mass to shift forward $140mm$. This occurs at approximately $(X, Y) = (-0.2, 4.5)m$. There is a time delay between the trigger activating and the drifting behavior. This time delay may be able to be reduced by adjusting the location of the shifting mass before and after the triggering event to minimize I_z. Other trajectories, such as a lane change maneuver, could have been used, but the simple circular trajectory was chosen to isolate the effects of the shifting mass.

Figure 11 shows the heading angle as a function of distance traveled. At just under 14m the mass is shifted to the front; however, drifting does not occur until just under 18m.

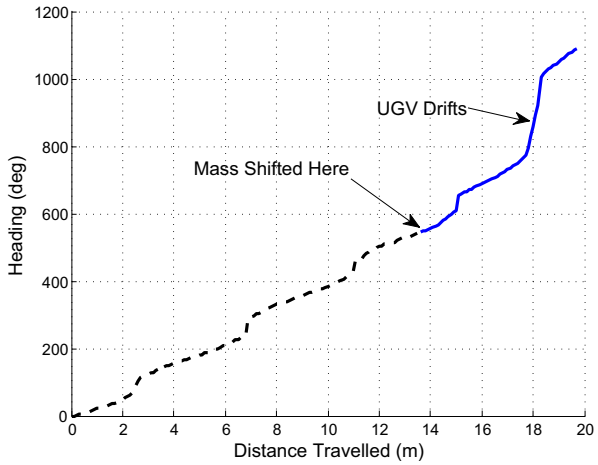

Fig. 11. Heading angle as a function of distance traveled.

IV. Conclusion and Future Work

A. Conclusions

This paper demonstrated that the agility of a UGV can be significantly improved with the addition of a DOF that allows the mass and inertial properties to be modified during operation. The internal mass shift modifies the vehicle/terrain interaction by changing the normal loading on each wheel, allowing the vehicle to execute a dynamic maneuver while maintaining a lower speed. The converse, creating a more stable vehicle, can also be achieved. Using both effects appropriately will yield a versatile, agile UGV capable of executing stable behavior on low coefficient of friction terrain at high velocities and extreme dynamic maneuvers at lower velocities than previously possible.

B. Future Work

Further investigation of the effects of loading on the dynamic properties of UGVs needs to be employed. Specifically, a better understanding of the tire properties is crucial. Future results will focus on an improved experimental system that can carefully and repeatably position the location of the center of mass multiple times during operation. That feature, coupled with more sophisticated position measurement system and feedback position control, will allow for a wider variety of experiments to be run. The future experimental UGV will also have independent velocity control for each of its rear wheels. This should further increase the dynamic capabilities of the vehicle. Additionally, continued examination of the control methods for such a vehicle is being performed.

V. Acknowledgments

The authors gratefully acknowledge Jeff Mizek and Sinan Oncu for their help conducting experiments and constructing the experimental UGV.

References

[1] P. Schenker, L. Sword, A. Ganino, D. Bickler, G. Hickey, D. Brown, E. Baumgartner, L. Matthies, B. Wilcox, T. Balch, H. Aghazarian, and M. Garrett. Lightweight rovers for mars science exploration and sample return. In *SPIE XVI Intelligent Robots and Computer Vision*, volume 3208, pages 24–36, 1997.

[2] C. Weisbin, G. Rodriguez, P. Schenker, H. Das, S. Hayati, E. Baumgartner, M. Maimone, I. Nesnas, and R. Volpe. Autonomous rover technology for mars sample return. In *Proceedings of the International Symposium on Artificial Intelligence, Robotics, and Automation in Space*, page 110, 1999.

[3] R. Altendorfer, N. Moore, H. Komsuoglu, M. Buehler, H. Brown Jr, D. McMordie, U. Saranli, R. Full, and D. Koditschek. Rhex: A biologically inspired hexapod runner. *Autonomous Robots*, 11:207, 2001.

[4] J. Clark, J. Cham, S. Bailey, E. Froehlich, P. Nahata, R. Full, and M. Cutkosky. Biomimetic design and fabrication of a hexapedal running robot. In *IEEE International Conference on Robotics and Automation*, volume 4, pages 3643–3649, 2001.

[5] T. Gillespie. *Fundamentals of Vehicle Dynamics*. Society of Automotive Engineers, 1992.

[6] R. Rajamani. *Vehicle Dynamics and Control*. Springer, 2006.

[7] M. Abdulrahim. On the dynamics of automobile drifting. *Society of Automotive Engineers Paper*, 2006-01-1019, 2006.

[8] B. E. Ilon. Wheel for a course stable self propelling vehicle movable in any direction, 1972. U.S. Patent 3,876,255.

[9] M. Yim, W.M. Shen, B. Salemi, D. Rus, M. Moll, H. Lipson, E. Klavins, and G. Chirikjian. Modular self-reconfigurable robot systems: Challenges and opportunities for the future. *IEEE Robotics and Automation Magazine*, March 2007.

[10] K. Iagnemma, A. Rzepniewski, S. Dubowsky, P. Priganian, T. Huntsberger, and P. Schenker. Mobile robot kinematic reconfigurability for rough-terrain. In *Proceedings of the SPIE International Symposium on Intelligent Systems and Advanced Manufacturing*, August 2000.